J. Electrochem. Sci. Eng. **16** (2026) 2975; https://doi.org/10.5599/jese.2975

Open Access : : ISSN 1847-9286
https://pub.iapchem.org/ojs/index.php/JESE

Original scientific paper

Mango peel extract as a green inhibitor in the corrosion of reinforced concrete

Alejandro Flores-Nicolás[1,✉], Elsa C. Menchaca-Campos[2] and Mario Flores-Nicolás[3]

[1]*Facultad de Ingeniería, Arquitectura y Diseño, Universidad Autónoma de Baja California, Carretera Transpeninsular Ensenada-Tijuana,3917, Playitas, 22860, Ensenada, B.C. México*
[2]*Centro de Investigación en Ingeniería y Ciencias Aplicadas, Universidad Autónoma del Estado de Morelos, Av. Universidad 1001, Cuernavaca C.P. 62209, MOR, México*
[3]*Instituto de Ciencias Básicas e Ingeniería, Universidad Autónoma del Estado de Hidalgo, Carr. Pachuca - Tulancingo Km. 4.5, Carboneras, 42184, Mineral de la Reforma, Hidalgo, Mexico*

Corresponding Authors: ✉*alejandro.flores25@uabc.edu.mx; Tel.: +52-777-376-1173*

Received: September 3, 2025; Accepted: March 24, 2026; Published: March 30, 2026

Abstract

Chloride-induced corrosion of reinforcing steel embedded in concrete is a problem that causes the elements to lose their physical and mechanical properties and can lead to premature failures in civil works. This research article analyses the effectiveness of the green corrosion inhibitor in cement paste through the ethanolic extract of mango peel. The materials were dosed with the inhibitor added to the mixing water and the mechanical properties of the material were analysed by manufacturing cylindrical test specimens. To understand the corrosion phenomena, cubic samples were prepared and immersed in a 3 % sodium chloride (NaCl) solution for 365 days, simulating a highly aggressive chloride-ion environment. Electrochemical techniques such as half-cell potential (HCP), electrochemical noise (EN), linear polarization resistance (LPR) and electrochemical impedance spectroscopy (EIS) are applied. The experimental results showed that the green corrosion inhibitor reduced the mechanical properties of concrete by 21.28 % compared to the blank, but a positive effect was observed in the corrosion evaluation. Initially, the inhibitor delayed the onset of corrosion, as indicated by high electrochemical noise and linear polarization resistance values due to the formation of a film of organic compounds present in the inhibitor extracts that acted on the active sites on the steel surface.

Keywords

Reinforcing steel; corrosion risks; localized corrosion; eco-friendly corrosion inhibitor; maceration; electrochemical techniques

Introduction

Corrosion of reinforcing steel in concrete is one of the main causes of durability problems in civil structures in coastal zones, due to aggressive saline environments. The composition of seawater considerably influences the corrosive behaviour of metals, specifically of steel bars in concrete, generating products such as oxides; as a result, strict corrosion monitoring policies are unavoidable [1].

Corrosion occurs due to the difference in chemical concentration of corrosive agents between different regions of the surface of steel, concrete and electrolyte, where an electrochemical cell is created [2]. The properties of steel and concrete are diminished by these damaging effects, so various prevention methods have been studied.

Currently, the use of green corrosion inhibitors provides sufficient corrosion protection even in the presence of high concentrations of aggressive chloride ions. In addition, they are biodegradable, non-toxic, environmentally friendly, inexpensive, and derived from renewable resources, with lower health and safety risks [3]. Therefore, many researchers have investigated environmentally friendly plant- and fruit-derived green inhibitors with different characteristics and bioactive compounds that mitigate the oxidation or reduction processes of steel in concrete. The diversity of eco-friendly corrosion inhibitors is really high, and many of them have the potential to be considered efficient and practical corrosion inhibitors in the field [4]. The inhibition efficiency of these materials depends on the stability of the formed chelate, and the inhibitor molecule must have centres capable of forming bonds with the metal surface by electron transport [5]. The inhibitory effect is mainly attributed to the –OH groups in aromatic substances, flavonoid rings and ascorbic acid, which interact both physically and chemically with the metal surface, forming a protective layer and increasing the resistance to Cl^- ions penetration [6].

Corrosion inhibitors are classified as anodic, cathodic or integrated inhibitors according to their mode of action [7]. Also, they can be analysed by different electrochemical techniques to achieve a thorough characterization and understand the corrosion mechanism, such as half-cell potential, electrochemical noise (EN), Pourbaix diagrams, linear polarization resistance and electrochemical impedance spectroscopy. By applying the above-mentioned methods, valuable information on the inhibitor composition and structure can be obtained, which is essential for understanding the related corrosion processes [8]. To contribute to the development of green corrosion inhibitors for reinforced concrete, mango peel extract was selected, continuing previous research. These inhibitors can be classified into inhibitors mixed into the cement paste and inhibitors applied on the surface [9]. Kennedy *et al.* [10] evaluated the corrosion potential using paste extracts of *Mangifera indica* (mango) resins layered to reinforce steel in concrete slabs. The results indicated a 10 % probability of corrosion, indicating that there is no, or very low probability of corrosion. Rahmani *et al.* [11] studied the influence of 2 wt.% mango extract, showing that it could reduce the metal corrosion rate in an aggressive solution by approximately 98 %. They demonstrated the spontaneous adsorption of heavy complex molecules (coordination compounds of extract molecules and inorganic cations) due to the negative adsorption energy. Asipita *et al*. [12] developed a sustainable corrosion inhibitor based on the plant extract of *Bambusa arundinacea*, which exhibited good adsorption characteristics and stabilized calcium silicate hydrates (C-S-H), thereby preventing the conversion of calcium hydroxide. Harb *et. al.* [13] valorised the extract of dried olive leaves as an inhibitor, obtaining an inhibition efficiency of 91.9 % with the methanolic extract. They also showed that the presence of compounds containing heteroatoms N and O with their p electrons is responsible for the corrosion inhibitory activity. Valdez-Salas *et al*. [14] evaluated the corrosion behaviour of a natural organic leaf extract of Neem and concluded that the inhibitor did not alter the integrity of the concrete or the

physicochemical parameters, achieving 95 % long-term corrosion protection after 182 days of evaluation. Al-Akhras Mashaqbeh [15], used herbal extracts from eucalyptus leaves as eco-friendly corrosion inhibitors in concrete reinforcement beams and prisms. They demonstrated that the extract has potential as an ecological corrosion inhibitor, as the corroded reinforced concrete beams showed that the amount of rust decreased with increasing concentration.

Generally, many studies have been conducted to understand and extend the service life of concrete structures and to assess the corrosion risks posed to steel in highly aggressive environments, but gaps remain. Therefore, the present research aims to develop new methods to mitigate corrosion in reinforced concrete. This article presents the novelty of a new, environmentally friendly inhibitor with a lower environmental impact compared to conventional inhibitors.

Experimental

Materials

For the preparation of the concrete paste, Portland cement CPC 30 R was used in accordance with the ASTM C 150 quality standard [16], crushed stone was used as coarse aggregate with a density of 2.70 g cm^{-3}, water absorption of 0.39 % and nominal maximum size of 1.9 cm. Sand is used as fine aggregate, with a nominal maximum size of 4.75 mm, density 2.47 g cm^{-3}, water absorption value of 2.13 % and fineness modulus of 2.33 [17]. In addition, corrugated steel construction rods and green mango peel inhibitor were used.

Preparations of the inhibitor

The mango fruits were collected from southern Mexico, then cleaned, and the fruit peel was dried at room temperature for 4 days, protecting it from sunlight. After that, the dry peel was crushed and ground into a fine powder. Mango peel extract was prepared using the maceration method with certain modifications, as described in [18].

The resulting fine powder was mixed with ethanol for 48 hours, after which the mixture was filtered through a filter paper. Finally, the excess cartridges were removed by pressure distillation using a rotary evaporator.

The structure of the ethanolic extract of mango peel contains O-H functional groups of phenols, aliphatic acids (C-H), carbonyl groups (C=O) and aromatic groups (C=C); these may be the functional groups that exist in the structure of gallic acid, mangiferin and iriflofenone from mango [19].

Proportion and preparation of the concrete paste

The green inhibitor solution was prepared first from a stock solution of 1000 ppm. 1.0 g of inhibitor was weighed using a Denver Instrument electronic balance with an accuracy of 0.1 mg, and then the inhibitor was dissolved in one litre of water.

A low concentration of 50 ppm was proposed to assess the inhibitor's effectiveness.

Table 1 shows the weights of materials for the white concrete mix and the concrete mix with an inhibitor at 50 ppm (CH-50).

Table 1. *Proportion of concrete components for 1 m^3*

	Blank [23]	CH-50
Cement content, kg	366.07	366.07
Water volume, l	197.65	187.77
Gravel content, kg	1047.65	1047.65
Sand content, kg	650.63	650.63
Inhibitor concentration, ppm	-----	50 (9.88 L)

It also details the amount of inhibitor (9.88 litres) in relation to the amount of reaction water in the concrete paste. The concrete mix was prepared at the desired concentration (50 ppm), and known quantities of the extract were added to the mixing water for the manufacture of cement paste, as shown in Figure 1.

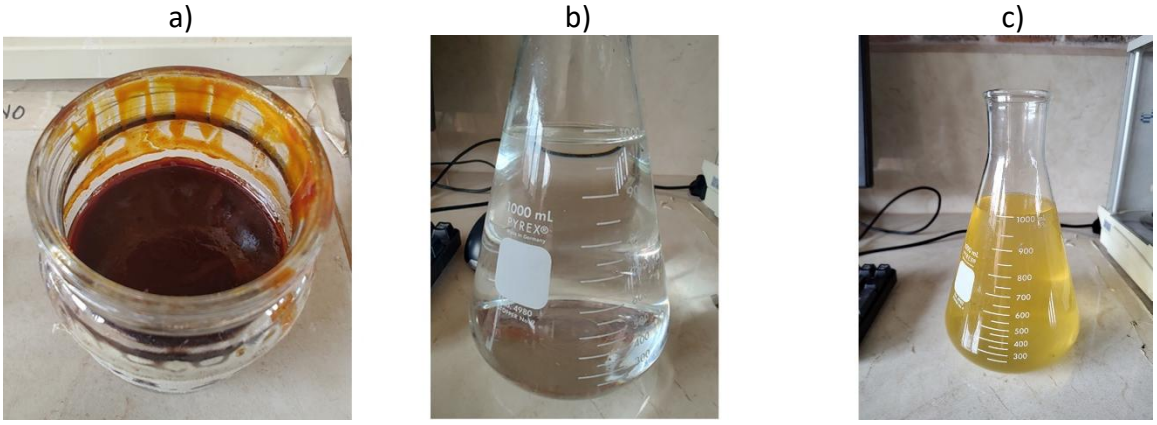

Figure 1 *Components of the green inhibitor of the ethanolic extract of mango: a) ethanolic extract of mango peel; b) water; c) green inhibitor*

Figure 2 shows the materials used for the preparation of the concrete. The materials were mixed as follows: first, gravel was added; then water and inhibitor; then sand; and finally, cement. All materials were stirred for 3 minutes in a Husky-brand industrial mixer with a 6.5 hp motor. Freshly mixed concrete was subjected to physical tests for slump and air content according to ASTM C143 and ASTM C231 standards [20,21]. The nomenclature used to identify the concrete samples was blank as control concrete, and CH-50 as concrete with inhibitor.

Figure 2. *a) Materials to produce concrete: gravel, sand, water, inhibitor and cement; b) concrete paste*

Sample preparation

For mechanical tests, 9 cylindrical probes with standard dimensions were made according to ASTM C 31 [22]. Compression tests were performed after 7 and 28 days of cylinder curing, using a 120-ton universal machine. For the electrochemical techniques, concrete cubes measuring 12 cm long, 8 cm wide and 12 cm high [23]. These specimens were placed in a 3 % sodium chloride saline solution, simulating marine conditions in coastal areas.

In addition, three corrugated construction steel rods, each with a diameter of 0.95 cm, were embedded as working electrodes (WE) at the interface between the paste and the steel. Teflon tape

was placed, protecting the steel bar from external moisture. The exposed area of the steel was 22.30 cm^2 [23].

Application of electrochemical techniques

Open circuit potential measurement

The tendency of any metal to react with its environment is indicated by the potential it develops in contact with it. On concrete reinforcement structures, the concrete acts as an electrolyte and the reinforcement will develop a potential depending on the concrete environment [24].

The corrosion potential, E_{corr} (rod/concrete half-cell), is measured as the potential difference (voltage) between the rod and the reference electrode (half-cell) [25]. The values obtained are recorded as the E_{corr} of the material, and these results can also be used to assess the degree of corrosion of the steel rods [26]. For steel corrosion potential measurements, the concrete cubes were monitored after 24, 48 and 72 hours immersed in the saline solution, to observe their trend and changes in potential. Subsequently, measurements are taken weekly for 365 days.

An electrochemical media cell was set up with a reference and working electrode (steel bars) connected to a multimeter; for this study, a saturated silver-silver chloride (Ag/AgCl) electrode was used as a reference according to ASTM C 876. Values below -150 mV are considered low corrosion with a 10 % probability; values between -150 and 300 mV are considered intermediate corrosion or a zone of uncertainty, and values below -300 mV are estimated to indicate severe corrosion with a 90 % probability of corrosion [23].

Electrochemical noise

When studying corrosion in reinforced concrete structures, electrochemical noise has many advantages because it is a non-destructive technique that does not alter the steel/concrete interface and is used to estimate the corrosion rate and the changes that the metal undergoes. The method is based on measurements of current and voltage fluctuations (electrochemical noise) generated by spontaneous charge flows during corrosion reactions [27]. A Gill AC-ACM Instruments-potentiostat was used to monitor electrochemical noise fluctuations in reinforced concrete. The electrochemical cell was composed of two working electrodes, and a third electrode was used as a counter electrode. In addition, an Ag/AgCl reference electrode closes the electrochemical cell. The equipment was configured for the test with 1024 data points with a sweep rate of 1 data point per second, leaving an interval of 30 mV. From this technique, the following data of interest for concrete structures can be obtained: corrosion rate through resistance to electrochemical noise (R_n), and type of corrosion occurring in the steel/concrete system.

For the calculation of resistance to electrochemical noise, Equation (1) was used [28]:

$$R_n = \frac{\sigma_V}{\sigma_I} \tag{1}$$

where R_n is resistance to electrochemical noise, σ_V is standard deviation of the potential and σ_I is standard deviation of the current.

R_n is considered equivalent to polarization resistance R_p and so, it can be related to the corrosion current by the Stern-Geary Equation (2):

$$R_p \text{ or } R_n = \frac{B}{j_{corr}} \tag{2}$$

where B is defined by Equation (3):

$$B = \frac{b_a b_c}{2.3\left(b_a + b_c\right)} \tag{3}$$

In Equations (2) and (3) R_p is in Ω or Ω cm², j_{corr} is the corrosion current in A or A cm^{-2}, and b_a and b_c are the Tafel constants in V dec^{-1} of current [28].

Other statistical parameters can be obtained from the electrochemical noise technique, such as the localization index (LI), which characterizes the type of corrosion present in the steel/concrete system. It is defined as the ratio between the standard deviation of the measured current (σ_I) and the root mean square (RMS) of the measured current and can be calculated from Equation (4):

$$\mathrm{LI} = \frac{\sigma_I}{\mathrm{RMS}} \tag{4}$$

The values of the LI are dimensionless; generalized corrosion ranges from 0.001 to 0.01, and mixed-type corrosion between 0.01 and 0.1. Localized corrosion shows values of 0.1 to 1. Subsequently, at the start of pitting in the steel bar, the values of LI are greater than 1.

Resistance to linear polarization

The linear polarization resistance (LPR) technique theoretically provides the corrosion current density and, therefore, the corrosion rate of steel by measuring the polarization resistance [29].

It is a non-destructive technique because it is generally applied at low voltages, allowing the current density (j_{corr}) to be measured. ASTM G 59–91 (Standard test method for potentiodynamic polarization resistance measurements) [30] defines the polarization resistance R_p as the slope of the current density Δj and potential ΔE curve as shown in Equation (5):

$$R_p = \frac{\Delta E}{\Delta j} \tag{6}$$

The calculation of the current density (j_{corr}) was performed by substituting R_n for R_p in Equation (3), resulting in Equation (7):

$$j_{corr} = \frac{B}{R_p} \tag{7}$$

where constant B is dependent on the anodic and cathodic Tafel slope constants calculated from Equation (3). In this work, a constant B of 26 mV was used, as this value is commonly used to describe corrosion phenomena in active steels [31].

For this measurement, a small voltage signal between -50 and +50 mV was applied relative to the corrosion potential (E_{corr}), according to the aforementioned standard. The sweep speed was 60 mV min^{-1}, and the resulting currents were recorded. R_p was obtained as the slope of potential *vs*. current density plots at $I = 0$, and j_{corr} was calculated using Equation (7).

According to Andrade and Alonso [32], a relationship can be established between j_{corr} values and the durability of reinforced concrete. A value of 0.1 μA cm^{-2} is considered negligible; a value in the range of 0.1 to 0.5 μA cm^{-2} is estimated to be moderate corrosion; values between 0.5 and 1.0 μA cm^{-2} are considered high corrosion; and values greater than 1 μA cm^{-2} indicate severe corrosion in the metal.

Electrochemical impedance spectroscopy

The resistance (or impedance) and frequency properties facilitate the determination of the corrosion state of reinforced concrete. Electrochemical impedance spectroscopy (EIS) or alternating current (AC) methods are applicable to sites that are difficult to analyse using a direct current (DC)

signal [33]. The ability to differentiate between closely related mechanisms makes electrochemical impedance spectroscopy (EIS) a powerful tool for such electrochemical studies [34].

The impedance measurements were performed at open-circuit potential (OCP) after 30 minutes of OCP stabilization, using a sinusoidal alternating current (AC) signal with an amplitude of 20 mV (peak-to-peak) and a frequency range from 10 kHz to 0.01 Hz. The inhibitor efficiency, (η / %), was calculated according to Equation (7):

$$\eta = \left(\frac{R_{ct(inh)} - R_{ct(0)}}{R_{ct(inh)}} \right) 100 \quad (8)$$

where $R_{ct\ (inh)}$ and $R_{ct\ (0)}$ are charge transfer resistance in the presence and absence of an inhibitor, which were obtained by a fitting procedure of the chosen EEC to measured impedance data.

Results and discussion

Effect of the slump test on concrete

Workability values of 14 cm were obtained for the blank concrete and 15 cm for the concrete with the green inhibitor. It can be observed that adding the green mango peel inhibitor significantly increases the slump compared to the white-mango peel inhibitor. This observation could be explained by the diffusion capacity of the corrosion inhibitor within the cement particles, which improves contact between the cement particles and water [35]. These results can be compared with those of other authors [36].

Effect of air content and porosity of concrete

Figure 3 shows the air content of the concrete in its fresh state and the material's porosity in its hardened state.

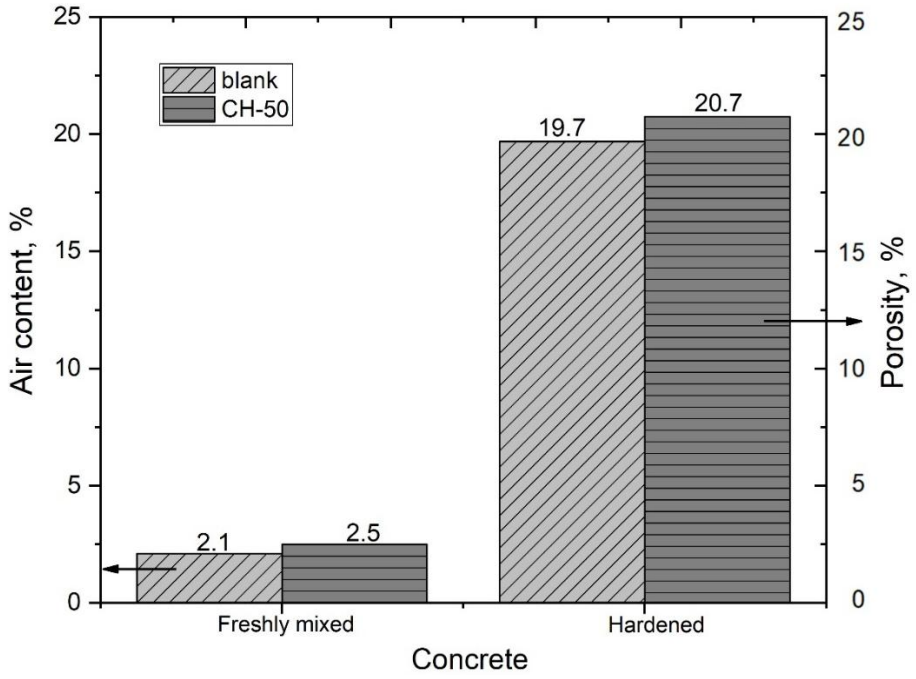

Figure 3. *Air content and porosity percentages of fresh and hardened concrete with and without inhibitor*

These physical properties are essential for evaluating the air voids trapped in the paste and the durability of the concrete. In other words, a greater number of voids in the cementitious matrix affects the final performance of the product's mechanical properties, and *vice versa*.

The air content and porosity increased for the samples with the green inhibitor, indicating that the green inhibitor led to poor internal curing of the concrete paste during cement hydration. Consequently, this leads to an increase in micropore diameter in hardened cement paste [12].

Furthermore, an increase in the material's permeability allows aggressive agents to penetrate the concrete matrix and interact with the reinforcing steel.

Compressive strength behaviour

Table 2 shows the values of the compressive strength (*f´c*) of the concrete and the standard separation of the samples. The blank presented a final resistance of 330.7 kg cm^{-2}, exceeding the proposed theoretical design of 300 kg cm^{-2}.

Table 2. *Compressive strength (f'c) values of concrete samples with and without inhibitor*

Nomenclature	*f'c* / kg cm^{-2}								Standard deviation (28 days), kg cm^{-2}
	7 days		28 days		7 days average		28 days average		
Blank	270.3	262.8	262.1	336.7	328.4	326.9	265.0	330.7	4.3
CH-50	215.5	207.6	209.0	257.7	267.3	255.9	210.8	260.3	5.0

During the first 7 days of curing, the CH-50 probe shows a lower *f´c* than the control sample, with an average of 210.8 kg cm^{-2}. This fact is a consequence of the cement paste's greater porosity. At the end of curing, the concrete showed a low compressive strength; the inhibitor affected the mechanical properties of the paste, with a 21.28 % decrease in the strength of the concrete after the introduction of the inhibitor extract. Low compressive strength values are due to increased porosity, which increases the penetration of aggressive chloride ions [9].

Interpretation of E_{corr} values

In general, organic inhibitors modify the potential between steel and water in the concrete pores, thereby forming a mechanical barrier against aggressive ions. The monitoring of the corrosion potential of the samples with inhibitor incorporation is shown in Figure 4.

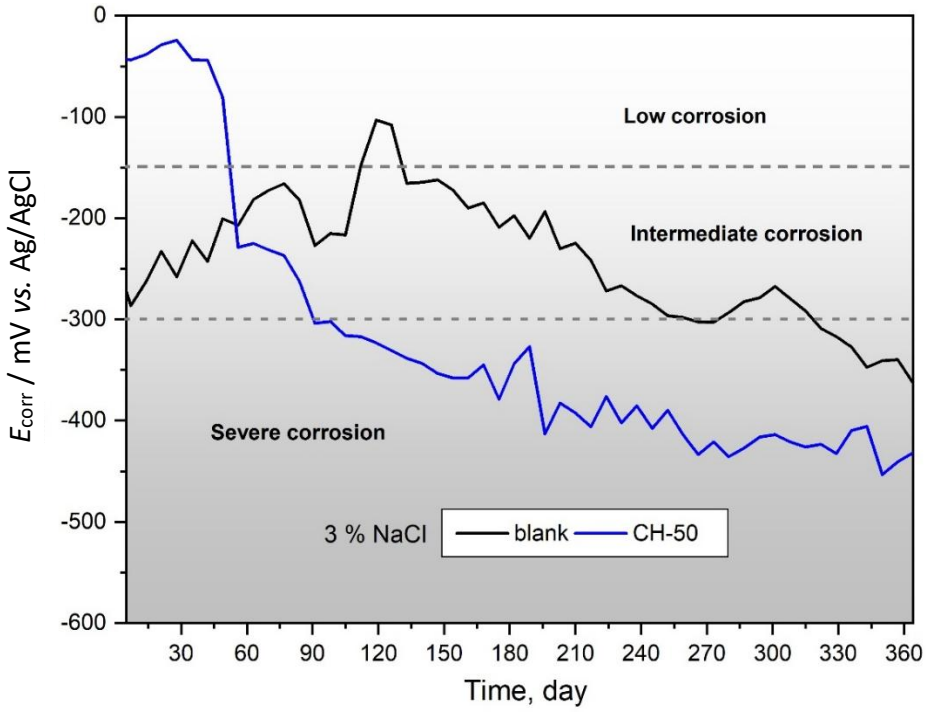

Figure 4. *Time change of corrosion potential of reinforced concrete samples in 3 % sodium chloride solution*

At an early age, specifically on day 7 of measurement, the CH-50 concrete sample shows less negative potentials than the control sample at -30 and -50 mV, entering a 10% probability of corrosion zone. The decrease in the samples' corrosion rate and the shift of the open-circuit potential toward the noble direction indicated that the samples reached a more noble state with immersion time [37]. This value indicates that the inhibitor delays the interaction of chloride ions within the cement paste.

Although organic inhibitors may contain one or more functional groups, many of them only delay the corrosion of steel in chloride and carbonate environments [38]. On day 56, a drop in potential occurs for the sample with the inhibitor. These parameters can be attributed to an increase in concrete permeability [39], indicating a higher concentration of chloride ions in the steel bar. Subsequently, more negative values of E_{corr} are observed in sample CH-50 during immersion, reaching a 90 % probability of corrosion from day 90 to day 365. This observation can be explained by the formation of metastable pits.

In Figure 5, the Pourbaix diagram [40] is shown, which summarizes the thermodynamic information of iron metal corrosion, delimiting between corrosion, immunity and passivation, and allows for evaluating the corrosion resistance under specific conditions. These diagrams indicate potential regions with respect to a standard hydrogen electrode (SHE*)* and the hydrogen potential (pH), showing where the metal corrodes and other regions where it is protected from corrosion [40].

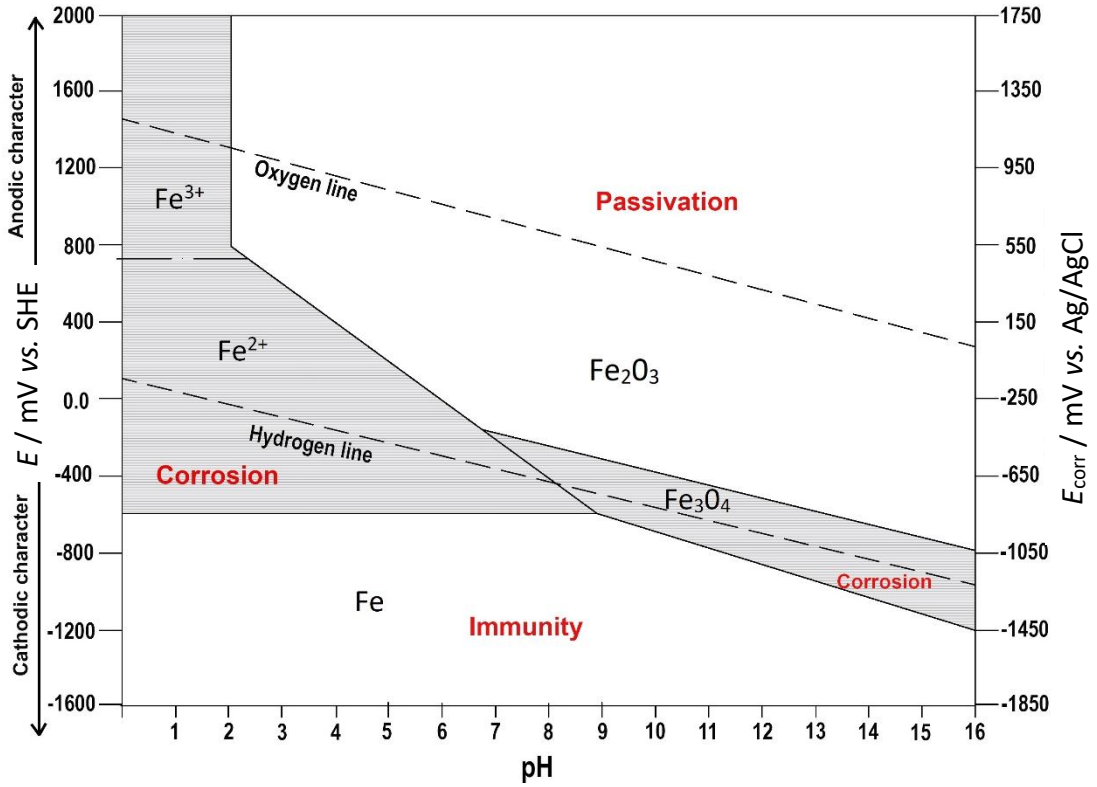

Figure 5. *Pourbaix equilibrium diagram for the analysis of corrosion of reinforced concrete*

It also shows the stability ranges of all species covered and can be used to predict reactions when combined with the redox potential of a given oxidizing or reducing agent. The Pourbaix diagram in Figure 5 provides a thermodynamic basis for assessing the corrosion potential of reinforced concrete. The different anodic and cathodic regions are identified. Furthermore, with corrosion potential data over 365 days in saline solution, values between -350 and -450 mV, it is evident that the sample is in a state of continuous ferric oxide (Fe_2O_3) formation. The species appear to be stable,

and the metal is protected by a thin surface oxide film on the steel surface. It should also be noted that the passivation indicated by the Pourbaix diagram depends on the pH of the concrete, but it does not describe the interaction of chloride ions at the steel/concrete interface. This information should be supplemented with other appropriate electrochemical techniques to obtain the reactions of the steel.

Interpretation of electrochemical noise values

The noise resistance results for the blank and the sample with the inhibitor are shown in Figure 6.

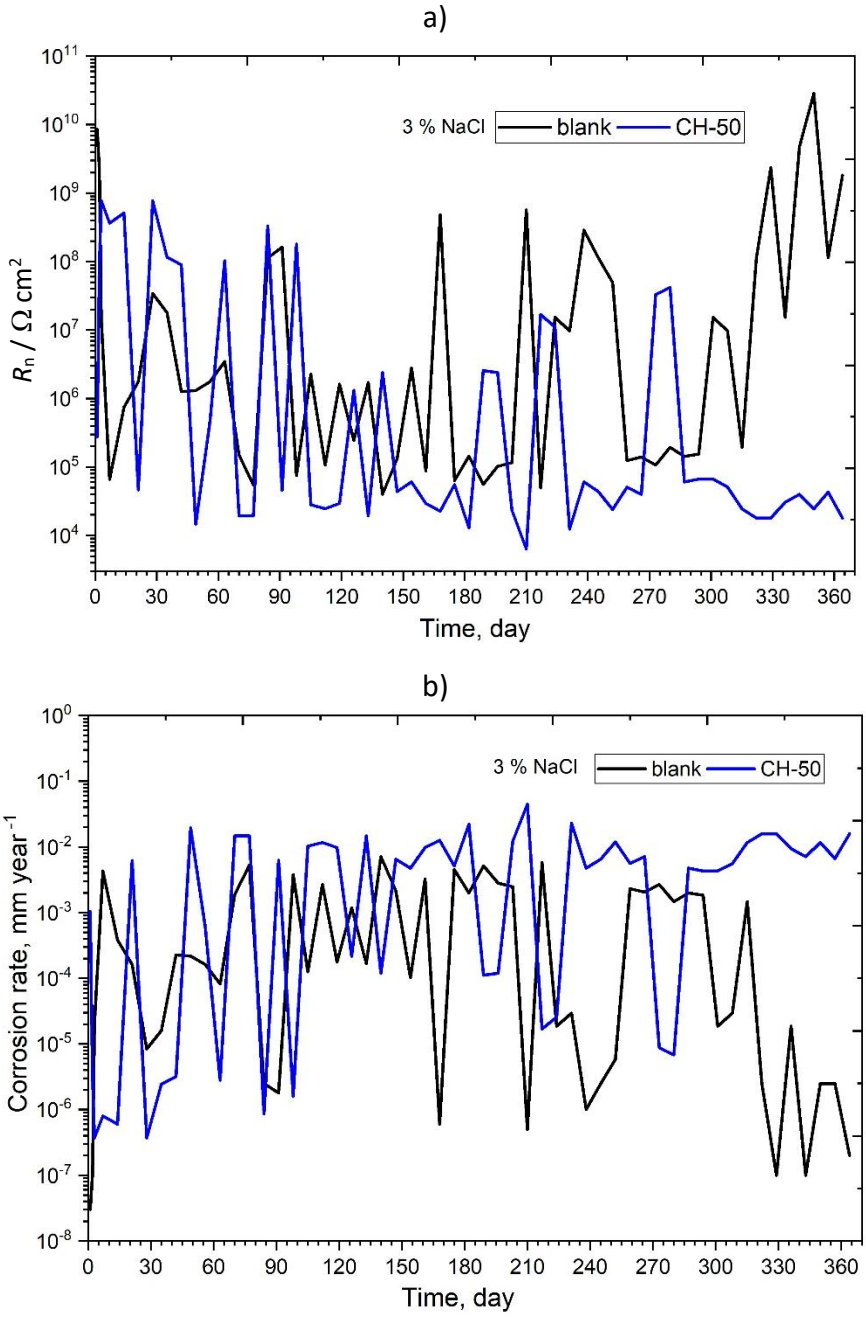

Figure 6. *a) Electrochemical noise resistance values and b) corrosion rates of reinforced concrete samples, measured during 365 days of exposure in saline solution*

In early measurements, high R_n values between 1000.0 and 0.1 MΩ cm^2 are observed for sample CH-50, indicating that steel is in a passive state. During the first few days and up to day 280, the CH-50 samples exhibit high and low fluctuations, indicating a breakdown of the passive layer and the

formation of a non-protective oxide film due to corrosion. The presence of mango ethanolic extract reduced the magnitude of these current transients, affirming its corrosion inhibition efficiency [41]. But as the monitoring time progressed, a drastic drop in R_n was observed on day 280, presenting values of 100 kΩ cm^2. This phenomenon indicates the accumulation of Cl^- ions at specific small points on the steel rod, leading to passive rupture events [42]. At the end of monitoring on day 365, the R_n decreased for the sample in the presence of the inhibitor, ranging from 100 to 10 kΩ cm^2. The drop in R_n could indicate that the concentration of chloride ions increases on the surface of the steel bar; consequently, the corrosion rate is severe, as shown in Figure 6 b).

Quantitative information on the corrosion rate of steel is of utmost importance for the evaluation of repair methods, predicting service life and for the structural evaluation of corroded elements. The type of corrosion present in the steel bars is localized, as shown in Figure 7.

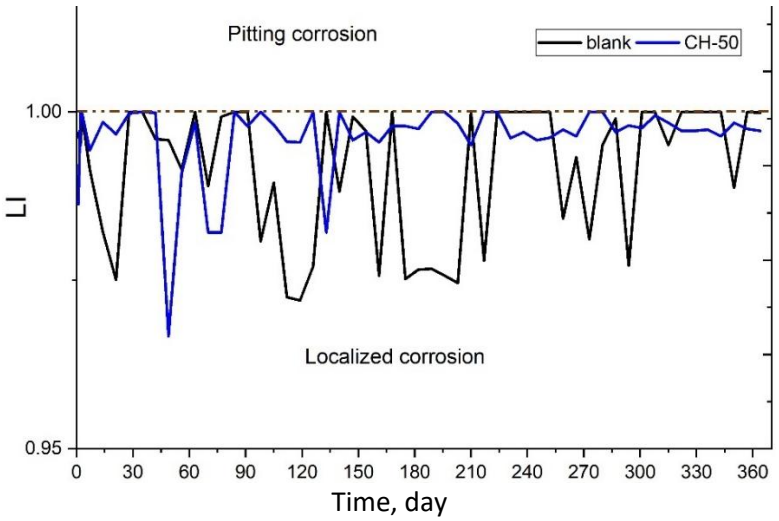

Figure 7. *Localization index values of reinforced concrete samples with and without inhibitor*

Linear polarization resistance measurement

The linear polarization resistance (LPR) results for the reinforced concrete samples containing inhibitor are detailed in Figure 8. During the beginning and up to day 70 of monitoring, high R_p values are observed for the sample with inhibitor values between 0.1 and 1 MΩ cm^2, indicating a low corrosion process of steel.

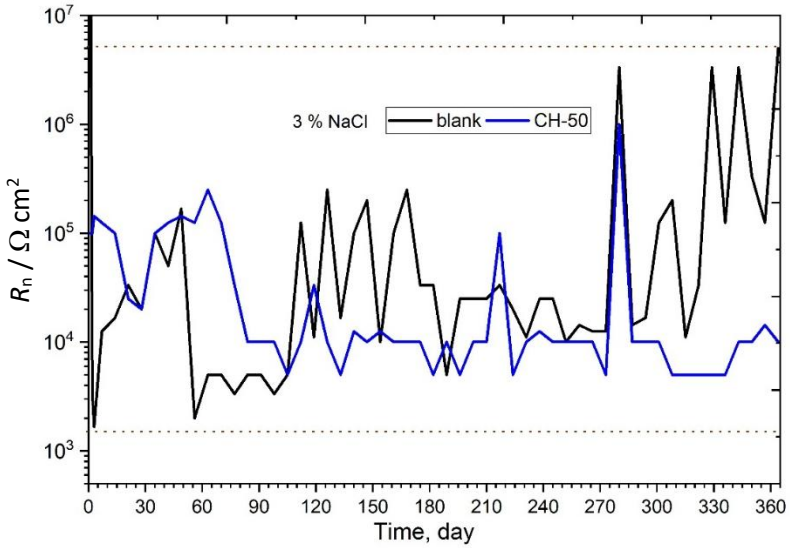

Figure 8. *Linear polarization resistance values of reinforced concrete samples during 365 days of exposure to saline solution*

The inhibitor shows a better response to steel corrosion at early times of exposure; the presence of mango extracts increases R_p, probably due to the adsorption of organic compounds in the extracts onto the active sites of the steel surface, thereby delaying both metal dissolution and hydrogen evolution reactions [43]. According to Asaad *et al.* [44], this is due to the slow diffusion of oxygen and Cl- ions through the pores of the concrete (capillary action) and to the insulating film component of the solid hydroxide layer at the steel/concrete interface, resulting from the adsorption of inhibitory compounds.

During day 80, a drop in R_p values is observed for sample CH-50, to about 10 kΩ cm^2, which remains almost constant until the end of the test. This phenomenon is due to the rupture of the dielectric film due to the high diffusion of aggressive agents such as Cl^-, O_2 and H_2O [45], because this sample presented larger voids in the cement matrix.

Figure 9 shows the durability of the concrete samples based on the current density (j_{corr}) values of the metal. CH-50 probes exposed to 365 days in the saline medium are observed to be in the high and very high corrosion ranges.

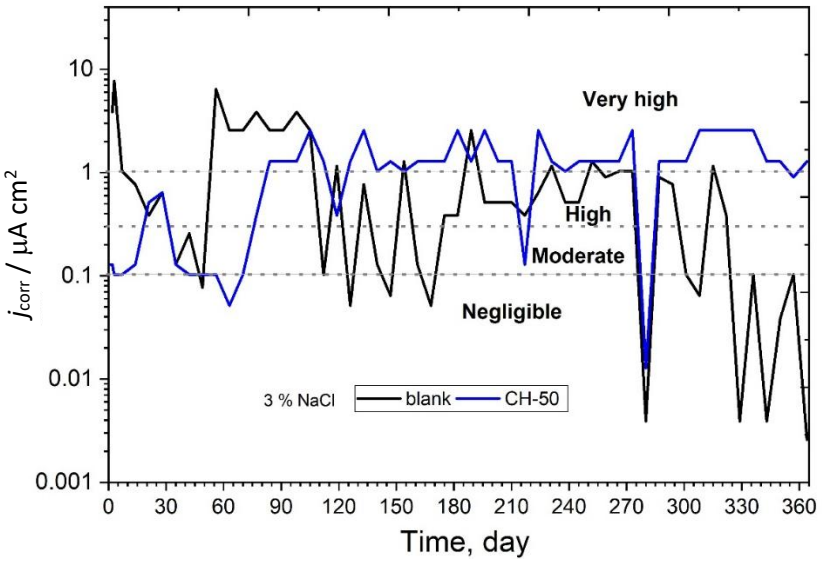

Figure 9. *Risk of damage to reinforcing steel in concrete samples under aggressive conditions of saline solution*

When the concentration of Cl^- ions exceeds a critical value, a drastic increase in the corrosion current occurred during the experiment [38]. The resistance decreases when the protective film is damaged under specific circumstances. These values indicate the onset of active corrosion of the reinforcing steel in the concrete and the formation of non-protective oxides on the metal surface, as reported by other authors [46].

Electrochemical impedance measurements of concrete

The EIS results for the blank concrete samples and those with the addition of the green inhibitor, mango peel extract, after 28 and 245 days of exposure to saline solution are shown in Figure 10.

To interpret the EIS data, we start from the measurements at the highest frequencies (10 to 1 kHz) and present them as "unfinished" capacitive loops. The high frequency point where $Z''=0$ is attributed to the strength of mass concrete, which represents the ohmic resistance of the solution in the pores or cracks of the cement matrix [23]. Subsequently, a second complete semicircle is generated at medium to low frequencies (1 kHz to 1 Hz). It is usually attributed to the corrosion film formed by the corrosion products.

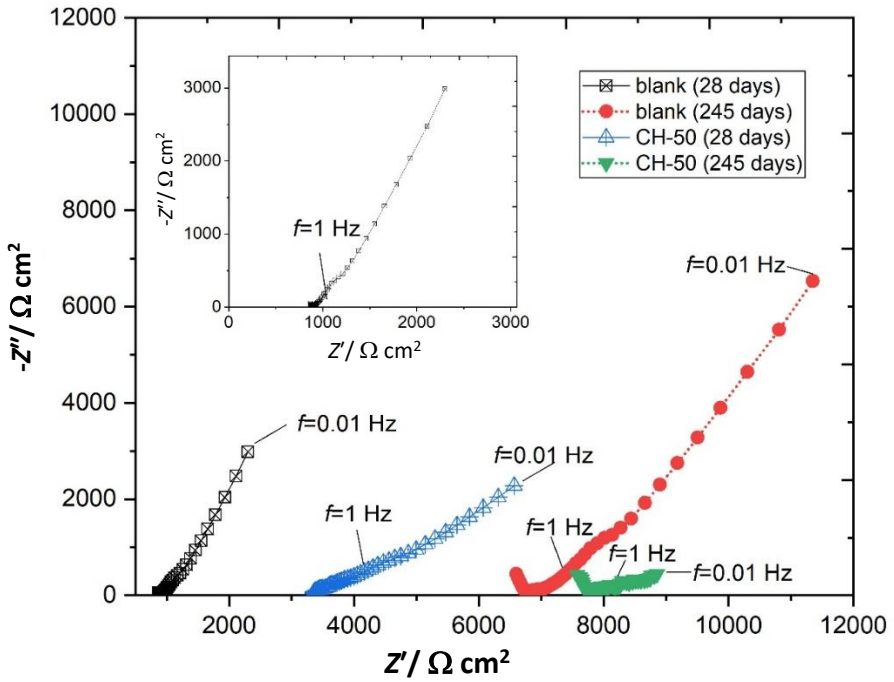

Figure 10. *Nyquist diagrams of blank and CH-50 concrete samples after 28 and 245 days of exposure to saline solution*

At low frequencies (1Hz to 0.01Hz), the third semicircle appears and is followed by prominent slope lines characteristic of diffusion impedance. This is usually ascribed to the interfacial region between steel and corrosion film, characterized by charge transfer resistance (R_{ct}) due to steel corrosion. In addition, diffusion effects can be ascribed to the diffusion of oxygen and free chloride ions into the concrete matrix, as was described by Herrera Hernandez *et al*. [47].

Likewise, a significant increase in R_s and some increase in R_{ct} are observed at higher exposure times, and for the sample with inhibitor, due to the larger radius of the capacitive rings at low frequencies, indicating a delay in the onset of corrosion of the reinforcing steel.

The sample with the inhibitor exhibits better electrochemical performance of the concrete at day 245; this is associated with the protection of the steel. Firstly, the formation of an organic film by the inhibitor covers small, localized corrosion points and prevents chloride ions from reaching the metal surface. It has been shown that increasing the solution resistance values prevents corrosive agents from reaching the steel embedded in the concrete [48], due to compounds present in the ethanolic extract of mango, such as phenols and carboxylic acids [49,50].

In Figure 11, the Bode diagrams (log of impedance modulus and phase angle *vs*. log *f*) are presented for the blank concrete samples and those with inhibitors. During the 28 days, sample CH-50 shows greater resistance to the solution. Likewise, greater resistance to polarization than the control sample, these values suggest the passivity of the system, i.e., a greater restriction on the flow of current [51]. The sample with the green inhibitor from mango extract maintained constant impedance values throughout the exposure, with a final value of 10 kΩ cm^2. These values are only slightly higher than the control sample, which explains a high corrosion rate.

Figure 12 illustrates the equivalent electrical circuit (EEC) used as a physical-conceptual model for the steel/concrete interface, based on the characteristics of the material and possibilities suggested in the literature [52]. The model consists of the solution resistance (R_s), followed by two time constants, CPEf and Rf, which represent the dielectric properties and ionic resistance of the protective film formed by the mango peel extract and the passive layer.

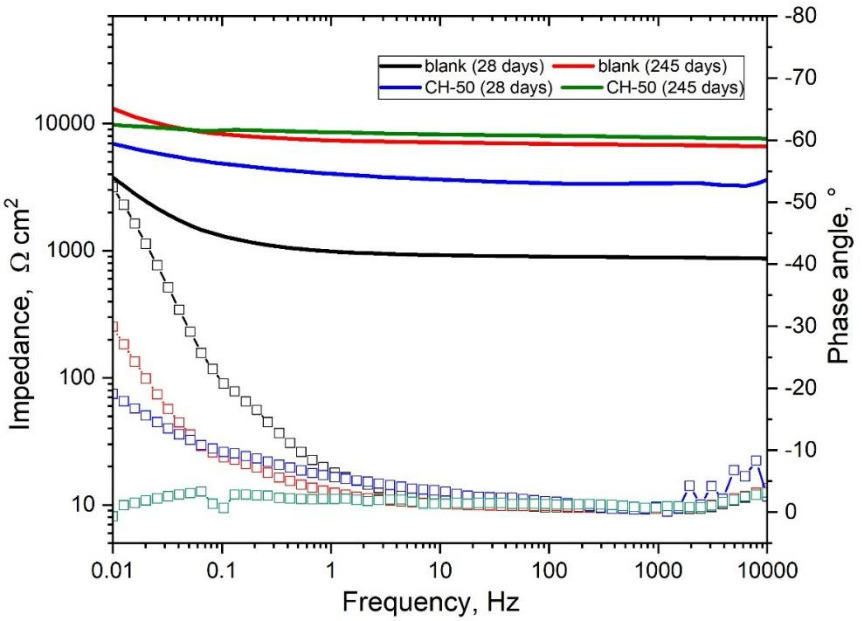

Figure 11. *Impedance modulus (up) and phase angle (down) plots for reinforced concrete specimens after 28 and 245 days of exposure to saline solution*

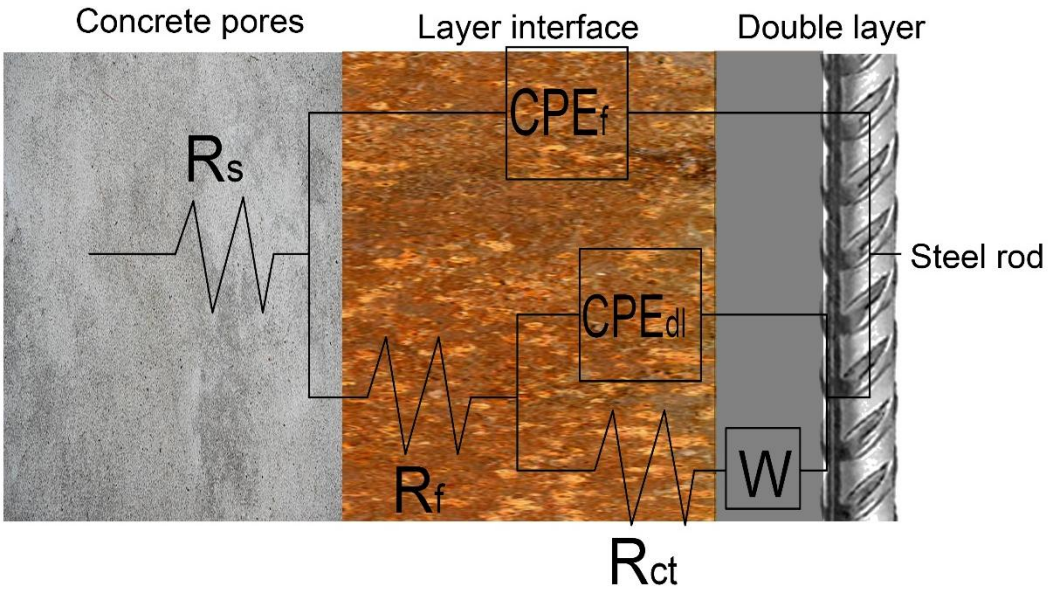

Figure 12. *Modified Randles equivalent circuit with 2-time constants for reinforced concrete*

CPE_{dl} and R_{ct} correspond to the electrochemical double layer and the resistance to charge transfer at the steel surface. Finally, a Warburg impedance (*W*) is included to account for diffusion-controlled processes of corrosive species through the concrete matrix and inhibitory film. This CEE provides a comprehensive framework for interpreting the increase in total impedance observed in the Nyquist plots (Figure 10) because of inhibitor adsorption.

Corrosion mechanism

The different electrochemical methods provide important parameters for understanding the behaviour of the metal embedded in the concrete. It is shown that the steel bar exhibits localized corrosion, with corrosion occurring at specific points across its total surface. In the Nyquist diagrams, the sample with inhibitor shows capacitive arcs of larger diameter than the control sample, and a straight line attributed to the diffusion part of the aggressive agents [33]. On day 245 of

measurement, the straight diffusion line decreases in slope, which is attributed to a transfer process in combination with mass transport of dissolved oxygen within the concrete.

According to Zomorodian and Behnood [4] and Pradityana *et al*. [53], organic inhibitory molecules, such as mango peel, which contains natural compounds and phenolic compounds, contribute significantly to the corrosion-inhibiting effect of mango peel extract by electrostatically adsorbing aggressive anions and thereby inactivating them.

Conclusions

The green inhibitor from ethanolic mango extract was incorporated into the reinforced concrete paste via the reaction water. From the experimental results, the following conclusions were derived:

The concrete paste's workability was not affected by the green inhibitor, but the inhibitor reduced compressive strength by increasing porosity in the cementitious matrix.

Corrosion potentials for concrete samples with a mango inhibitor showed better performance, delaying chloride diffusion for 90 days and achieving a low-to-intermediate corrosion state.

The concrete sample with inhibitor (CH-50) showed high noise and polarization resistance values (Rn and Rp) at the beginning of the measurements, but these values decreased toward the end of the experiment, leading to an increase in the corrosion rate of reinforcing steel.

The useful life level in the steel/concrete system with the green inhibitor showed a moderate-to-high corrosion level, with j_{corr} greater than 0.5 µA cm^{-2}.

The corrosion rate of the reinforcing steel was localized throughout the measurement period, from the first days of exposure to the saline environment until the end of exposure, with localization index values between 0.1 and 1.

The green inhibitor showed a positive effect on aggressive agents (such as Cl^- ions) compared to the blank during the first days of the experiment, as indicated by Nyquist and impedance data, thereby delaying the onset of corrosion.

Recommendations

For future research, the authors could recommend conducting experiments with the mango peel inhibitor at concentrations above 50 ppm, specifically 100, 200, 500 or 1000 ppm, and to perform the complete analysis of mechanical and electrochemical properties of the reinforced concrete. Other environmentally friendly corrosion inhibitors prepared by different type of maceration could also be studied

Acknowledgements: *The authors express their gratitude to the Universidad Autonoma de Baja California (UABC), the Centro de Investigación en Ingeniería y Ciencias Aplicadas (CIICap), and the Secretaría de Ciencia, Humanidades, Tecnología e Innovación (Secihti).*

Conflict of interest: *The authors declare no conflicts of interest.*

References

[1] A. Shokri, M. S. Fard, Corrosion in seawater desalination industry: A critical analysis of impacts and mitigation strategies, *Chemosphere* **307** (2022) 135640. https://doi.org/10.1016/j.chemosphere.2022.135640

[2] A. Shokri, An investigation of corrosion and sedimentation in the air cooler tubes of benzene drying column in linear alkyl benzene production plant, *Chemical Papers* **73** (2019) 2265-2274. https://doi.org/10.1007/s11696-019-00776-z

[3] A. K. Badawi, I. S. Fahim, A critical review on green corrosion inhibitors based on plant extracts: Advances and potential presence in the market, *International Journal of Corrosion and Scale Inhibition* **10** (2021) 1385-1406. https://dx.doi.org/10.17675/2305-6894-2021-10-4-2
[4] A. Zomorodian, A. Behnood, Review of corrosion inhibitors in reinforced concrete: Conventional and green materials, *Buildings* **13** (2023) 1170. https://doi.org/10.3390/buildings13051170
[5] A. Kadhim, A. A. Al-Amiery, R. Alazawi, M. K. S. Al-Ghezi, R. H. Abass, Corrosion inhibitors, A review. *International Journal of Corrosion and Scale Inhibition* **10** (2021) 54-67. https://dx.doi.org/10.17675/2305-6894-2021-10-1-3
[6] L. Casanova, F. Ceriani, E. Messinese, L. Paterlini, S. Beretta, F. M. Bolzoni, M. Pedeferri, Recent Advances in the Use of Green Corrosion Inhibitors to Prevent Chloride-Induced Corrosion in Reinforced Concrete, *Materials* **16** (2023) 7462. https://doi.org/10.3390/ma16237462
[7] A. Shokri, Reinforced concrete corrosion; Mechanism, challenges, prospective, and future roadmap, *Journal of Electrochemical Science and Engineering* **15** (2025) 2820. https://doi.org/10.5599/jese.2820
[8] A. Shokri, M. Sanavi Fard, Under deposit corrosion failure: mitigation strategies and future roadmap, *Chemical Papers* **77** (2023) 1773-1790. https://doi.org/10.1007/s11696-022-02601-6
[9] S. P. Palanisamy, G. Maheswaran, A. G. Selvarani, C. Kamal, G. Venkatesh, Ricinus communis–A green extract for the improvement of anti-corrosion and mechanical properties of reinforcing steel in concrete in chloride media, *Journal of Building Engineering* **19** (2018) 376-383. https://doi.org/10.1016/j.jobe.2018.05.020
[10] C. Kennedy, F.O. Philip-Kpae, T.A. Nadum, Corrosion Potential Assessment of Ecofriendly Inhibitors Layered Reinforcement Embedded in Concrete Structures in Severe Medium, *International Journal of Scientific & Engineering Research* **9** (2018) 1590-1607. https://www.researchgate.net/publication/325103001_Corrosion_Potential_Assessment_of_Ecofriendly_Inhibitors_Layered_Reinforcement_Embedded_in_Concrete_Structures_in_Severe_Medium
[11] M. H. Rahmani, A. Dehghani, M. Salamati, G. Bahlakeh, B. Ramezanzadeh, Mango extract behavior as a potent corrosion inhibitor against simulated chloride-contaminated concrete pore solution; coupled experimental and computer modeling studies, *Journal of Industrial and Engineering Chemistry* **130** (2024) 368-381. https://doi.org/10.1016/j.jiec.2023.09.040
[12] S. A. Asipita, M. Ismail, M. Z. Abd Majid, Z. A. Majid, C. Abdullah, J. Mirza, Green Bambusa Arundinacea leaves extract as a sustainable corrosion inhibitor in steel reinforced concrete, *Journal of Cleaner Production* **67** (2014) 139-146. https://doi.org/10.1016/j.jclepro.2013.12.033
[13] M. B. Harb, S. Abubshait, N. Etteyeb, M. Kamoun, A. Dhouib, Olive leaf extract as a green corrosion inhibitor of reinforced concrete contaminated with seawater, *Arabian Journal of Chemistry* **13** (2020) 4846-4856. https://doi.org/10.1016/j.arabjc.2020.01.016
[14] B. Valdez-Salas, R. Vazquez-Delgado, J. Salvador-Carlos, E. Beltran-Partida, R. Salinas-Martinez, N. Cheng, M. Curiel-Alvarez, *Azadirachta indica* leaf extract as green corrosion inhibitor for reinforced concrete structures: corrosion effectiveness against commercial corrosion inhibitors and concrete integrity, *Materials* **14** (2021) 3326. https://doi.org/10.3390/ma14123326
[15] N. Al-Akhras, Y. Mashaqbeh, Potential use of eucalyptus leaves as green corrosion inhibitor of steel reinforcement, *Journal of Building Engineering* **35** (2021) 101848. https://doi.org/10.1016/j.jobe.2020.101848

[16] ASTM C150-07 Standard Specification for Portland Cement (2012) https://doi.org/10.1520/C0150-07
[17] A. F. Nicolás, M. F. Nicolás, E. C. M. Campos, J. U. Chavarín, Mechanical Behavior of Concrete Reinforced with Natural Palm and Mango Fibers, *Journal of Engineering and Technological Sciences* **57** (2025) 48-65. https://doi.org/10.5614/j.eng.technol.sci.2025.57.1.4
[18] A. N. Adilah, B. Jamilah, M. A. Noranizan, Z. N. Hanani, Utilization of mango peel extracts on the biodegradable films for active packaging, *Food Packaging and Shelf Life* **16** (2018) 1-7. https://doi.org/10.1016/j.fpsl.2018.01.006
[19] M. Ramezanzadeh, G. Bahlakeh, Z. Sanaei, B. Ramezanzadeh, Corrosion inhibition of mild steel in 1 M HCl solution by ethanolic extract of eco-friendly *Mangifera indica* (mango) leaves: electrochemical, molecular dynamics, Monte Carlo and ab initio study, *Applied Surface Science* **463** (2019) 1058-1077. https://doi.org/10.1016/j.apsusc.2018.09.029
[20] ASTM C143/C143M-12 Standard Test Method for Slump of Hydraulic-Cement Concrete. (2015). https://doi.org/10.1520/C0143_C0143M-12
[21] ASTM C231-09a Standard Test Method for Air Content of Freshly Mixed Concrete by the Pressure Method. (2010). https://doi.org/10.1520/C0231-09A
[22] ASTM C31/C31M-23 Standard Practice for Making and Curing Concrete Test Specimens in the Field. (2024). https://doi.org/10.1520/C0031_C0031M-23
[23] A. Flores Nicolás, E. C. Menchaca Campos, M. Flores Nicolás, J. J. Martínez González, O. A. González Noriega, J. Uruchurtu Chavarín, Influence of Recycled High-Density Polyethylene Fibers on the Mechanical and Electrochemical Properties of Reinforced Concrete, *Fibers* **12** (2024) 24. https://doi.org/10.3390/fib12030024
[24] H. W. Song, V. Saraswathy, Corrosion monitoring of reinforced concrete structures–a review, *International Journal of The Electrochemical Science* **2** (2007) 1-28. https://doi.org/10.1016/S1452-3981(23)17049-0
[25] C. Andrade, I. Martínez, Techniques for measuring the corrosion rate (polarization resistance) and the corrosion potential of reinforced concrete structures, in: *Non-Destructive Evaluation of Reinforced Concrete Structures,* Woodhead Publishing, 2010, pp. 284-316. https://doi.org/10.1533/9781845699604.2.284
[26] A. Flores-Nicolás, M. Flores-Nicolás, J. Uruchurtu-Chavarín, Corrosion effect on reinforced concrete with the addition of graphite powder and its evaluation on physical-electrochemical properties, *Revista ALCONPAT* **11** (2021) 18-33. https://doi.org/10.21041/ra.v11i1.501
[27] J. M. Smulko, K. Darowicki, A. Zieliński, Evaluation of reinforcement corrosion rate in concrete structures by electrochemical noise measurements, *Russian Journal of Electrochemistry* **42** (2006) 546-550. https://doi.org/10.1134/S1023193506050132
[28] D. Mills, P. Lambert, S. Yang, Electrochemical noise measurement to assess corrosion of steel reinforcement in concrete, *Materials* **14** (2021) 5392. https://doi.org/10.3390/ma14185392
[29] A. Clément, S. Laurens, G. Arliguie, F. Deby, Numerical study of the linear polarisation resistance technique applied to reinforced concrete for corrosion assessment, *European Journal of Environmental and Civil Engineering* **16** (2012) 491-504. https://doi.org/10.1080/19648189.2012.668012
[30] ASTM G59-23, Standard Test Method for Conducting Potentiodynamic Polarization Resistance Measurements. (2023). https://doi.org/10.1520/G0059-23
[31] A. F. Nicolás, E. C. M. Campos, M. F. Nicolás, O. A. G. Noriega, C. A. G. Pérez, J. U. Chavarín, Corrosion resistance of reinforcing steel in concrete using natural fibers treated with used engine oil, *Civil Engineering Journal* **10** (2024) 1012-1033. https://doi.org/10.28991/CEJ-2024-010-04-02

[32] C. Andrade, C. Alonso, Test methods for on-site corrosion rate measurement of steel reinforcement in concrete by means of the polarization resistance method, *Materials and Structures* **37** (2004) 623-643. https://doi.org/10.1007/BF02483292
[33] J. K. Kim, S. H. Kee, C. M. Futalan, J. J. Yee, Corrosion monitoring of reinforced steel embedded in cement mortar under wet-and-dry cycles by electrochemical impedance spectroscopy, *Sensors* **20** (2019) 199. https://doi.org/10.3390/s20010199
[34] M. Sánchez, J. Gregori, C. Alonso, J. J. García-Jareño, H. Takenouti, F. Vicente, Electrochemical impedance spectroscopy for studying passive layers on steel rebars immersed in alkaline solutions simulating concrete pores, *Electrochimica Acta* **52** (2007) 7634-7641. https://doi.org/10.1016/j.electacta.2007.02.012
[35] D. T. Tran, H. S. Lee, J. K. Singh, H. M. Yang, M. G. Jeong, S. Yan, A. K. Singh, Effects of Hybrid Corrosion Inhibitor on Mechanical Characteristics, Corrosion Behavior, and Predictive Estimation of Lifespan of Reinforced Concrete Structures, *Buildings* **15** (2025) 1114. https://doi.org/10.3390/buildings15071114
[36] S. Ghoreishiamiri, P. B. Raja, M. Ismail, N. H. Roslan, S. F. Hashemi Karouei, Mechanical properties of contaminated concrete inhibited by Areca catechu leaf extract as a green corrosion inhibitor, *Asian Journal of Civil Engineering* **21** (2020) 1355-1367. https://doi.org/10.1007/s42107-020-00283-7
[37] G. Sahoo, R. Balasubramaniam, On the corrosion behaviour of phosphoric irons in simulated concrete pore solution, *Corrosion Science* **50** (2008) 131-143. https://doi.org/10.1016/j.corsci.2007.06.017
[38] I. B. Topçu, A. Uzunömeroğlu, Properties of corrosion inhibitors on reinforced concrete, *Journal of Structural Engineering & Applied Mechanics* **3** (2020) 93-109. https://doi.org/10.31462/jseam.2020.02093109
[39] S. A. Abdulsada, T. I. Török, Studying chloride ions and corrosion properties of reinforced concrete with a green inhibitor and plasticizers, *Structural Concrete* **21** (2020) 1894-1904. https://doi.org/10.1002/suco.201900580
[40] E. McCafferty, *Thermodynamics of corrosion: Pourbaix diagrams,* in *Introduction to Corrosion Science,* Springer New York, 2009. pp. 95-117. https://doi.org/10.1007/978-1-4419-0455-3_6
[41] I. B. Obot, I. B. Onyeachu, A. Zeino, S. A. Umoren, Electrochemical noise (EN) technique: review of recent practical applications to corrosion electrochemistry research, *Journal of Adhesion Science and Technology* **33** (2019) 1453-1496. https://doi.org/10.1080/01694243.2019.1587224
[42] A. Flores-Nicolás, M. Flores-Nicolás, E. C. Menchaca Campos, J. Uruchurtu-Chavarín, Study on Corrosion of Reinforced Concrete with Synthetic Fiber Using Electrochemical Noise Technique, *Civil and Environmental Engineering* **28** (2025) 271-281. https://doi.org/10.2478/cee-2025-0021
[43] O. D. Onukwuli, M. Omotioma, Optimization of the inhibition efficiency of mango extract as corrosion inhibitor of mild steel in 1.0 M H_2SO_4 using response surface methodology, *Journal of Chemical Technology and Metallurgy* **51** (2016) 302-314. https://www.researchgate.net/publication/303128448_Optimization_of_the_inhibition_efficiency_of_mango_extract_as_corrosion_inhibitor_of_mild_steel_in_10M_H2SO4_using_response_surface_methodology
[44] M. A. Asaad, M. Ismail, M. M. Tahir, G. F. Huseien, P. B. Raja, Y. P. Asmara, Enhanced corrosion resistance of reinforced concrete: Role of emerging eco-friendly Elaeis guineensis/silver nanoparticles inhibitor, *Construction and Building Materials* **188** (2018) 555-568. https://doi.org/10.1016/j.conbuildmat.2018.08.140
[45] B. Da, H. Yu, H. Ma, Z. Wu, Reinforcement corrosion research based on the linear polarization resistance method for coral aggregate seawater concrete in a marine

environment. *Anti-Corrosion Methods and Materials* **65** (2018) 458-470. https://doi.org/10.1108/ACMM-03-2018-1911

[46] M. A. Pech-Canul, P. Castro, Corrosion measurements of steel reinforcement in concrete exposed to a tropical marine atmosphere, *Cement and Concrete Research* **32** (2002) 491-498. https://doi.org/10.1016/S0008-8846(01)00713-X

[47] H. H. Hernández, F. G. Díaz, G. D. J. Fajardo San Miguel, J. C. V. Altamirano, C. O. G. Morán, J. M. Hernández, Electrochemical impedance spectroscopy as a practical tool for monitoring the carbonation process on reinforced concrete structures, *Arabian Journal for Science and Engineering* **44** (2019) 10087-10103. https://doi.org/10.1007/s13369-019-04041-z

[48] M. A. Asaad, G. F. Huseien, M. H. Baghban, P. B. Raja, R. Fediuk, I. Faridmehr, F. Alrshoudi, Gum arabic nanoparticles as green corrosion inhibitor for reinforced concrete exposed to carbon dioxide environment, *Materials* **14** (2021) 7867. https://doi.org/10.3390/ma14247867

[49] E. S. Endah, V. Saraswaty, D. Ratnaningrum, W. Kosasih, A. Ardiansyah, C. Risdian, H. Setiyanto, Phyto-assisted synthesis of zinc oxide nanoparticles using mango (Mangifera indica) fruit peel extract and their antibacterial activity, *IOP Conference Series: Earth and Environmental Science* **1201** (2023) 012081. https://doi.org/10.1088/1755-1315/1201/1/012081

[50] R. Thivagaran, N. Salim, N. H. A. Bakar, Ethanolic Mangifera Indica Leaves Extract as Green Corrosion Inhibitor, *Journal of Advanced Research in Applied Sciences and Engineering Technology* **29** (2023) 228-234. https://doi.org/10.37934/araset.29.3.228234

[51] F. G. D. Silva, J. B. L. Liborio, A study of steel bar reinforcement corrosion in concretes with SF and SRH using electrochemical impedance spectroscopy, *Materials Research* **9** (2006) 209-215. https://doi.org/10.1590/S1516-14392006000200018

[52] H. S. Magar, R. Y. Hassan, A. Mulchandani, Electrochemical impedance spectroscopy (EIS): Principles, construction, and biosensing applications, *Sensors* **21** (2021) 6578. https://doi.org/10.3390/s21196578

[53] A. Pradityana, Subowo, A. Anzip, D. M. Soedjono, E. Widiyono, R. Prayogi, Inhibition mechanism on mango peels as organic inhibitor in 1 M HCl solution, *AIP Conference Proceedings* **1983** (2018) 050018. https://doi.org/10.1063/1.5046291